4.4 ESTIMATION OF SCALING PARAMETERS AND ENERGY FLUXES OVER THE GULF OF MEXICO USING NEW OBSERVATIONS AND USING THE COARE PROGRAM

Clinton P. MacDonald*, Paul T. Roberts, and Charles A. Knoderer
Sonoma Technology, Inc., Petaluma, California

Steven R. Hanna
Hanna Consultants, Kennebunkport, Maine

1. INTRODUCTION

There is a need to calculate the transport and dispersion of pollutants emitted from offshore oil and gas exploration and production activities in the Gulf of Mexico to estimate and understand their impact on onshore areas. However, much uncertainty exists concerning the atmospheric boundary layer in the region due to space and time variations caused by variable underlying water temperatures and the effects of mesoscale atmospheric structures. The current study, supported by the U.S. Department of the Interior Minerals Management Service, has instrumented six oil platforms to obtain boundary layer observation measurements, including 915-MHz radar wind profilers, 2-KHz Radio Acoustic Sounding Systems (RASS), and near-surface routine meteorology instruments. Two of these meteorological stations operated from May 1998 through September 2001 and four operated from October 2000 through September 2001. The profilers measure winds and RASS measure virtual temperatures between heights of about 100 m and a few kilometers. The near-surface observations at the oil platforms include sea-skin temperature as well as wind speed, wind direction, air temperature, and mixing ratio at a reference elevation, z_r, of about 25 m. These new data, in addition to the traditional data collected by buoys and available from the National Climatic Data Center (NCDC), are being analyzed to investigate the overwater surface energy balance and boundary layer structure for both steady-state horizontally homogeneous conditions and for conditions variable in time and space. These three-dimensional, time-dependent fields will be used for analysis of transport and dispersion from overwater sources. Figure 1 shows a map of the Gulf of Mexico region and indicates the locations of the various observation sites.

The Tropical Ocean-Global Atmosphere Coupled-Ocean Atmosphere Response Experiment (TOGA COARE) marine boundary layer algorithms (Fairall et al., 1996) are being used to calculate a three-year climatology of hourly-averaged and/or monthly-averaged fundamental boundary layer scaling parameters such as the surface roughness length (z_o), the friction velocity (u*), the scaling temperature (T*), the scaling water vapor mixing ratio (q*), and the Monin-Obukhov length (L), in addition to the latent and sensible heat fluxes. The outputs of the COARE program (e.g., boundary layer scaling parameters and energy fluxes) are being compared to observations and to simulations by the Eta numerical weather prediction model.

2. BACKGROUND ON THE COARE MODEL

The basic structure of the COARE marine boundary layer model is an outgrowth of the Liu-Katsaros-Businger (LKB) method (Liu et al., 1979). The COARE algorithm was designed to improve estimates of surface fluxes and scaling parameters over the deep ocean in tropical regions (Fairall et al., 1996). The original version of COARE was released in 1993, and three new COARE versions have been released since the current study began. Version 2.5b, released in May 1997, included updated transfer coefficients. Version 2.6b was released in January 2000. There are six relatively minor differences between versions 2.5b and 2.6b, including changing the Charnook "constant" to a parameter based on wind speed data from Hare et al. (1999) and Yelland and Taylor (1996). An improved version of COARE (version 2.6bw) was released in June 2000. An important difference between version 2.6bw and the prior versions is that version 2.6bw incorporates surface gravity wave information, based on wave height and period data. This change should increase the accuracy of the estimates of surface fluxes and scaling parameters over shallow areas since the characteristics of waves differ from the deep ocean to the shallow coastal waters.

In addition to the changes in the COARE program by its original authors, additional changes to the program were made for this project with guidance and approval from one of its authors, Dr. Christopher Fairall. There was an occasional problem with the evaporative cooling calculation due to unrealistically high amounts of solar energy being estimated to reach the ocean surface. The representation in the COARE follows from laboratory measurements with artificial light sources and ignores the fact that the solar flux reaching the surface of the ocean has been partially absorbed by the atmosphere. In the equation for the net absorption by the ocean (Equation 1 below), the first coefficient was changed from 0.137 to 0.060, based on tests performed by Dr. Fairall. This change gave a more realistic representation of the actual

* *Corresponding author address*: Clinton P. MacDonald; Sonoma Technology, Inc., 1360 Redwood Way, Suite C, Petaluma CA 94954; e-mail: clint@sonomatech.com

absorption, which caused the evaporative cooling calculations to better agree with observations.

Net = SW*(.137+11*CST -6.6e-5/ CST*(1-exp (-CST/8.0e-4))) (1)

Where
Net = Net absorption by the ocean
SW = Incoming short wave radiation
CST= cool skin thickness

During early daylight hours, under light-wind conditions and with the air temperature warmer than sea temperature (i.e., a stable vertical temperature gradient), COARE calculated unrealistic sea-skin temperature from the under-water temperature. This was caused by a lack of heat removal due to the very small accumulated stress (surface momentum flux) and very thin (almost zero) warm layer thickness of the ocean surface. To solve this problem, a minimum stress of .002 N/m^2 was imposed for this calculation only. This value was chosen after analysis of measured stresses during TOGA-COARE (verbal communication with Dr. Fairall, July 2002).

3. APPLICATION OF THE COARE MODEL

The COARE model requires the following input data: time and site location; wind speed, air temperature, and relative humidity (RH) within the surface layer at reference height z_r; sea surface skin temperature (T_s) or sea temperature near the surface plus radiation estimates; and mixing height. If the near-surface sea temperature is used, then solar and downwelling longwave radiation fluxes need to be estimated from some alternate source in order to correct this temperature to a skin temperature. Precipitation data is not required, but if available, can be used by COARE to estimate the precipitation contribution to the energy balance equation. Wave height and period data are not required but have been used in this project to account for the different wave structures, which improves the accuracy of the estimates of surface fluxes and scaling parameters over shallow ocean areas, such as the Gulf of Mexico.

Data were acquired and processed from the following sites: 1998 and 2001 offshore buoy data from seven sites, shoreline C-MAN station data from five sites, and data collected as part of this project on the Vermillion (VRM) and South Marsh Island (SMI) oil platforms. Figure 1 shows the locations of the offshore buoys, the C-MAN stations, and the VRM and SMI platforms. The figure also shows monitoring sites from the Breton Island Aerometric Monitoring Program; data from these sites will be included in future analyses.

The C-MAN stations are located in very shallow water on the coast. Since the COARE model is not currently designed to use data collected in such areas, the data from these sites were used only in test exercises to evaluate how COARE would respond compared to open-water sites. The data collected at the VRM and SMI platforms meet the COARE input data requirements. The data collected at buoys meet most of the COARE data requirements, with the exception of solar and longwave radiation which were not observed. Instead, radiation fluxes were estimated using six-hourly ETA model cloud simulations and sun elevation data to calculate the water skin temperatures from water temperatures at depths of about 0.5 to 1.0 m.

4. RESULTS

The climatological part of the study is discussed first. Using the hourly meteorological data collected from May 1998 through October at 12 sites, hourly sensible heat flux, latent heat flux, surface stress, frictional velocity, temperature and relative humidity scaling parameters, z_r/L, and roughness length were calculated using COARE 2.5bw. Monthly statistics were then calculated from these hourly values. Monthly averages were not computed if more than 25% of the data in a given month were missing. In addition, averages were calculated for each surface flow direction class defined as onshore, offshore, parallel east, and parallel west.

The case study part of the analysis is discussed second. In this analysis, time series of hourly averages of selected meteorological and derived boundary layer parameters were created using COARE version 2.6bw, for periods in January, March, July, and October 2000. The analysis included comparisons of derived outputs from COARE with simulations of the Eta model for sensible and latent heat flux and friction velocity. The Eta model simulations were available on a six-hourly basis out to 48 hours. Since the Eta model runs every 12 hours, there are four sets of simulations available at any given hour; therefore, the COARE-derived data for any given hour and parameter were compared to four separate Eta model simulations.

4.1 Monthly Averages

The fluxes and scalar parameters calculated by the COARE algorithm in the Gulf of Mexico are physically consistent with expectations and are similar to observations and COARE calculations for TOGA, which took place in the warm western Pacific Ocean near the equator. Calculated monthly average sensible heat fluxes (Figure 2) in the Gulf of Mexico are about 5 to 30 w/m^2, typical of other over-water sites. Similarly, calculated monthly average latent heat fluxes (Figure 3) are about 50 to 150 w/m^2, also typical of other over-water sites. Both the latent and sensible heat fluxes are higher in the late fall and winter and are lowest in the summer although the yearly cycle in latent heat values is less pronounced. These observations are consistent with the light winds and smaller sea skin-to-air temperature differences in the summer compared to the other times of the year (see Figures 4 and 5, respectively). Calculated monthly average sensible heat fluxes are about one-fifth of the calculated monthly average latent heat fluxes, and the differences were generally greatest in the summer and less in the late fall and winter.

The monthly average calculated total heat flux (sensible plus latent) is in fair agreement (within a factor of two) among the sites in the Gulf of Mexico (Figure 6). However, the calculated total heat flux at VRM is often 2 to 3 times lower than at SMI and other buoy sites during the winter and early spring and is more similar to the C-MAN sites, GDIL1 and SRST2. The difference between VRM and the other sites is driven by lower calculated latent heat fluxes, which drives both smaller u* and smaller humidity scaling parameters.

The monthly average ETA model latent and sensible heat fluxes (Figure 7 and 8) are generally in good agreement with the calculated fluxes. However, the model fluxes do not show as great a variation among sites as the calculated fluxes. In addition, the model fluxes are about 20% greater than the calculated fluxes in the fall and early winter but are very similar during spring and summer.

The COARE-calculated monthly average friction velocity, u* (Figure 9), shows agreement among the sites well within a factor of two and often within 20%. This agreement is important because u* is the key scaling velocity for estimating transport speeds and dispersion rates. The calculated u* is slightly lower from May through August and peaks in late fall and early winter. The monthly average ETA model friction velocity (Figure 10) shows the same yearly pattern as the calculated friction velocity. However, the ETA model friction velocity is about 10 to 20% higher than the calculated friction velocity in the fall and early winter. This is most likely why the ETA model fluxes are high during the same period.

Monthly average air temperatures agree among sites (Figure 11). The temperatures are warmest in July and August (about 28.5°C) and coolest in the winter (ranging from about 12.5°C to 21°C). The air temperatures show greater difference between near-shore and offshore sites in winter compared to summer. This is probably due to cold fronts influencing near-shore sites more than offshore sites. For example, the average monthly air temperature at offshore buoys 42001 and 42002 is about 21°C in January and 28°C in August. On the other hand, the average monthly temperatures at the near-shore sites, VRM and SRST2, are about 12.5°C in January and 28.5°C in August.

Like the monthly average air temperatures, sea-skin temperatures are warmest in July and August and coolest in January and show a site grouping similar to air temperatures (Figure 12). The far offshore sea-skin temperatures at buoys 42001 and 42002 show the least amount of seasonal variation (about 6°C) compared to the near-shore sites (about 17.5°C maximum at VRM between September and January). The magnitude of fluxes generally follows the annual variation of the sea-skin temperature, with maxima in late fall and minima in late spring.

The differences between sea-skin minus air temperature are, on average, about +1 to +3°C at most sites all year (Figure 5). The difference is less in late spring and greater in late fall and early winter. This persistent positive temperature difference has been noted by Dr. Fairall at most other sites located on warm water oceans.

Scalar monthly average wind speed shows good agreement among sites (Figure 4). The lowest speeds occur in July and August and the highest in December and January. There is a transition between lower wind speeds in August to higher winds speeds in September. Review of weather maps indicates that the high wind speeds in September are probably a result of tropical storms and the high wind speeds in October are a result of strong continental winds or Bermuda Highs.

Relative humidity agrees among sites and is about 75% during all months.

4.2 Flow Direction Averages

The sensible heat fluxes (Figure 13) increase as wind speed increases and the sea-skin minus air temperature difference increases. The figure shows that sensible heat flux is maximized for northerly offshore flow directions, which are more likely to be marked by above-average wind speeds and by relatively low air temperatures. The sensible heat flux is lowest for onshore flow directions, when the boundary layer is in balance with the water surface. The average difference in sensible heat flux for offshore and onshore flow directions across the nine stations is about a factor of 10. There are some differences among the sites but they are not consistent and the reasons are not obvious.

The average latent heat fluxes (Figure 14) show some differences at most sites between offshore and onshore wind directions. The latent heat flux is largest during offshore (northerly) flows, which tend to be associated with “post-trough” synoptic conditions, higher wind speeds, and relatively low dew points that follow a cold front. In fact with any kind of offshore flow, the dew point in the air is likely to be less than that usually found over the water. The minimum latent heat fluxes on the figure occur with onshore flows.

The friction velocity, u*, (Figure 15) is calculated by COARE using the log wind profile relation. Since that relation has u* proportional to u, then the largest u* values are associated with high-wind periods, which tend to occur during offshore wind directions. There is a slight minimum in u* during parallel west wind directions. There is relatively little variability in u* from site to site.

The surface roughness (Figure 16) over water is a function of wind speed, wave height, and period; therefore, the roughness would be expected to be larger during flow directions with stronger winds. This is the case for the seven buoy sites in Figure 16 since

the largest wind speeds and, therefore, the largest roughnesses, are found for offshore flow directions; however, there are no clear variations at the oil platform and C-MAN sites.

Wind speed, u, (Figure 17) is the only parameter in this section that is observed at all sites. It is not calculated by COARE. Its total range in the figure is from 4 m/s for onshore flow at GDIL1, to 7.5 m/s for offshore flows at BURL1. At most sites, the maximum occurs during offshore flows, which may be associated with post-cold front conditions from the north quadrant.

5. RESULTS OF CASE STUDIES

Time series of hourly averaged observations, COARE-model calculations, and Eta-model simulations of boundary layer parameters at the observing sites in the Gulf of Mexico were analyzed for four five-day periods in January, March, July, and October, 2000. Data from January 20-25 from buoy 42040 are discussed here in order to illustrate the analysis methods and typical results. As seen in Figure 1, buoy 42040 is located several tens of km to the southeast of the Mississippi River delta.

5.1 Meteorological Observations

The time series of observed air and water temperatures and wind speed are plotted in Figure 18, showing large variations in wind and air temperature during these five days with air temperatures 5 to 10°C cooler than the water temperatures for the first two days and for the last day and a half. Wind speeds were moderate to strong (about 5 to 15 m/s) during these periods. However, during the middle of the time period, the air warmed slowly to approach and even exceed the water temperature for over 12 hours. The winds dropped to nearly zero just before a frontal passage at about 3 a.m. on January 24, after which the air temperature dropped 5°C in an hour and wind speed rapidly increased to 16 m/s.

5.2 Sensible Heat Fluxes

Figure 19 shows the COARE-calculated and Eta-simulated sensible heat fluxes during this time period. The COARE model is using the buoy-observed meteorological variables and is seen to produce very large (for the ocean) fluxes with magnitudes of about 150 w/m^2 during the beginning and ending periods, when the water-air temperature differences were very large (5 to 10°C) and the wind speeds were high (about 10 to 15 m/s). However, during the 12- to 15-hour period in the middle of the time series, when the air temperature exceeded the water temperature, the COARE-calculated sensible heat fluxes were negative (i.e., toward the water surface) with magnitudes of about 10 w/m^2. The Eta model simulations of sensible heat flux are only about 30% larger than the COARE-calculated values during the periods with large air-water temperature differences. However, during the middle period, the Eta model simulates positive (upward) sensible heat fluxes although they are small (about 0 to 20 w/m^2). This tendency exists for all sites and periods. That is, occasionally the site shows periods with observed air temperatures warmer than water temperatures, leading to COARE-calculated negative heat fluxes, while the Eta model simulates positive (but small) heat fluxes. During the late spring, when the air temperature is observed to be greater than the water temperature about 20 to 40% of the time, long periods of mismatches can occur in the signs of the COARE- and Eta-simulated sensible heat fluxes.

5.3. Latent Heat Fluxes

Figure 20 shows the COARE-calculated and Eta-simulated latent heat fluxes during this same time period (January 20-25, 2000). Relatively large latent heat fluxes of about 500 w/m^2 are calculated by both COARE and Eta for the periods near the beginning and end of the five days. This is the same magnitude as the solar heat flux on a summer day. These large sensible heat fluxes are due to the large air-water temperature differences and the moderate wind speeds. Figure 3 illustrates that, even in January, the Gulf of Mexico water temperature is still fairly warm—about 21°C—allowing large latent heat fluxes to occur.

During the 12- to 18-hour period on January 23, when the air temperature slightly exceeded the water temperature and winds dropped, COARE-calculated latent heat fluxes dropped as low as 20 w/m^2.

The Eta-model simulations in Figure 20 are seen to approximately track the COARE calculations, with differences of about 30% during the two periods with high fluxes. During the period with small fluxes, the Eta simulations roughly bracket the COARE calculations. No relation is evident between the age of the Eta simulation and agreement with the COARE curve on the figure.

6. FURTHER STUDIES

As stated in the introduction, the data collection phase of this study ended in fall 2001. At the present time, the data are still being analyzed. Many types of data have not been discussed in this paper, such as those from 915-MHz wind profilers and RASS. These analyses are in progress. The purpose of the current paper has been to illustrate the types of data that have been collected and the types of analyses being carried out.

Many issues still need study, such as the usefulness of the C-MAN (coastal) observation sites in the COARE algorithm. We are also studying the meaning of the Eta analyzed fields (EDAS) and to what extent the observations are used in developing those fields. The ultimate goal is to have an optimum set of three-dimensional time-dependent meteorological variables over the Gulf of Mexico for use in air quality simulations. For example, these data could be used to assess the impacts of emissions from oil platforms on the Breton Island National Wildlife Refuge, which is a “Class I” area in the EPA priority scheme.

ACKNOWLEDGMENTS

This research was sponsored by the Minerals Management Service of the U.S. Department of Interior. The authors appreciate the support of the Technical Contract Monitor, Dr. Chester Huang. The authors also appreciate the technical advice from Dr. Christopher Fairall, the developer of the COARE model, and the assistance given by numerous persons responsible for meteorological data collection on the oil platforms.

REFERENCES

Fairall, C.W., E.F. Bradley, D.P. Rogers, J.B. Edson, G.S. Young, 1996: Bulk parameterization of air-sea fluxes for TOGA COARE. *J. Geophys. Res.* **101**, 3747-3764.

.

Hare, J.E., P.O.G. Persson, C.W. Fairall, and J.B. Edson, 1999: Behavior of Charnock's relationship for high wind conditions. Proc. 13th Symposium of Boundary Layers and Turbulence. AMS. Dallas, TX, Jan. 15-20, paper 5B.8.

Liu, W.T, K.B. Katsaros and J.A. Businger, 1979: Bulk parameterization of the air-sea exchange of heat and water vapor including the molecular constraints at the interface, *J. Atmos. Sci.* **36**, 1722-1735.

Taylor, P.K., and M.J. Yelland, 2000: The dependence of sea surface roughness on the height and steepness of the waves. *J. Phys. Oceanography*, **31**, 572-590.

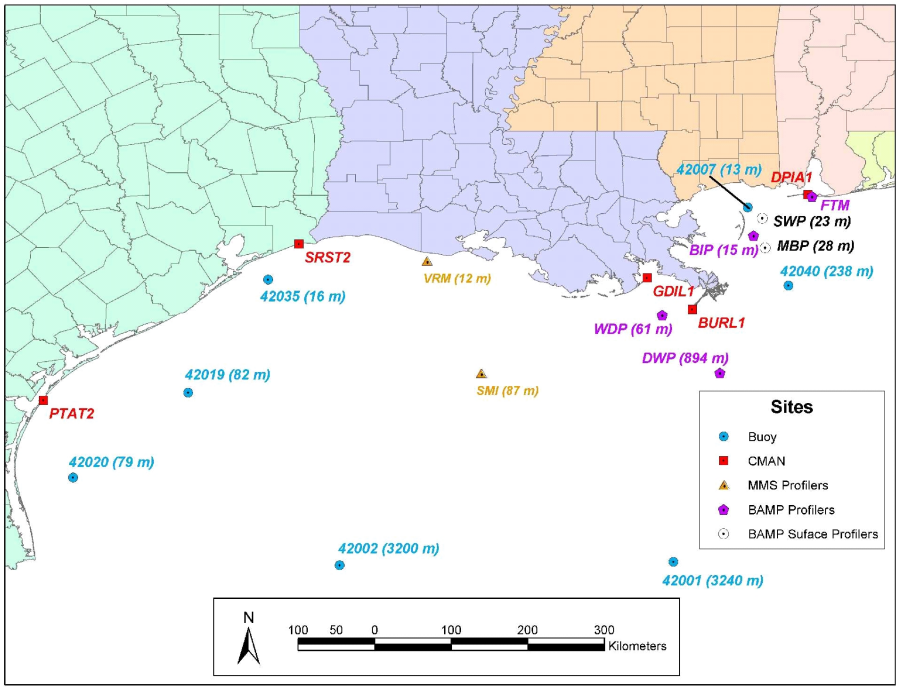

Figure 1. Meteorological Stations in the Gulf of Mexico study domain.

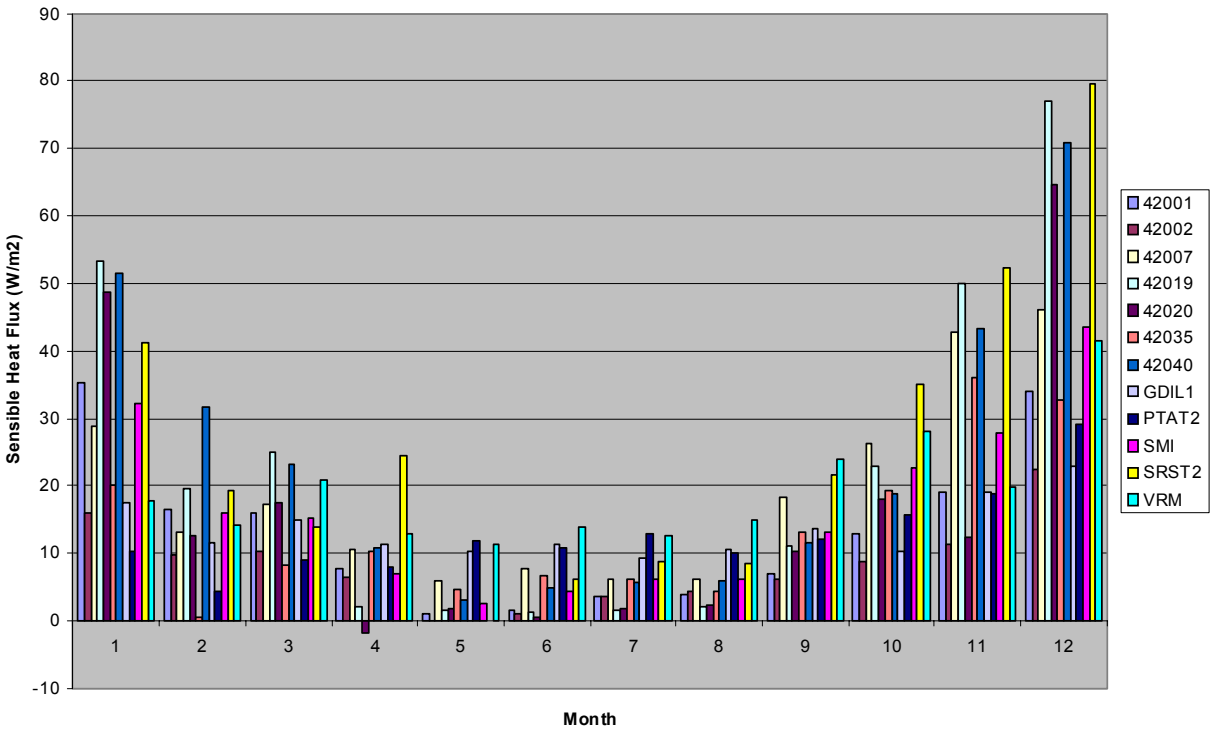

Figure 2. COARE monthly average sensible heat fluxes for May 1998 through October 2001.

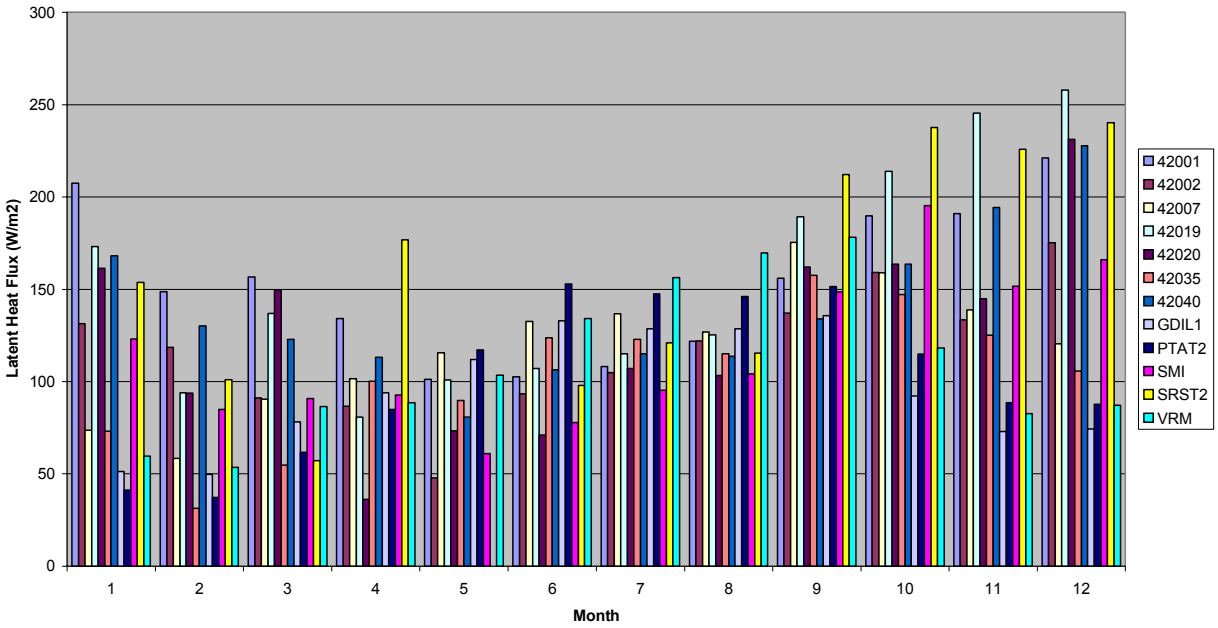

Figure 3. COARE monthly average latent heat fluxes for May 1998 through October 2001.

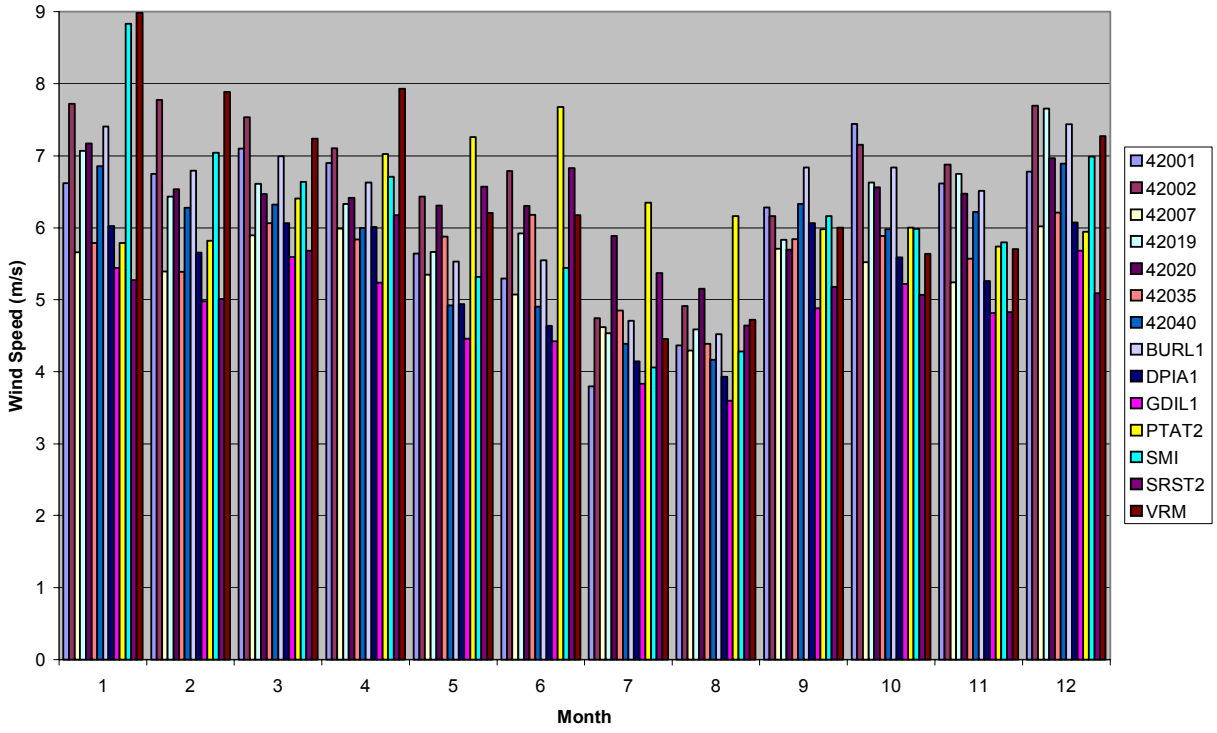

Figure 4. Observed monthly average wind speed for May 1998 through October 2001.

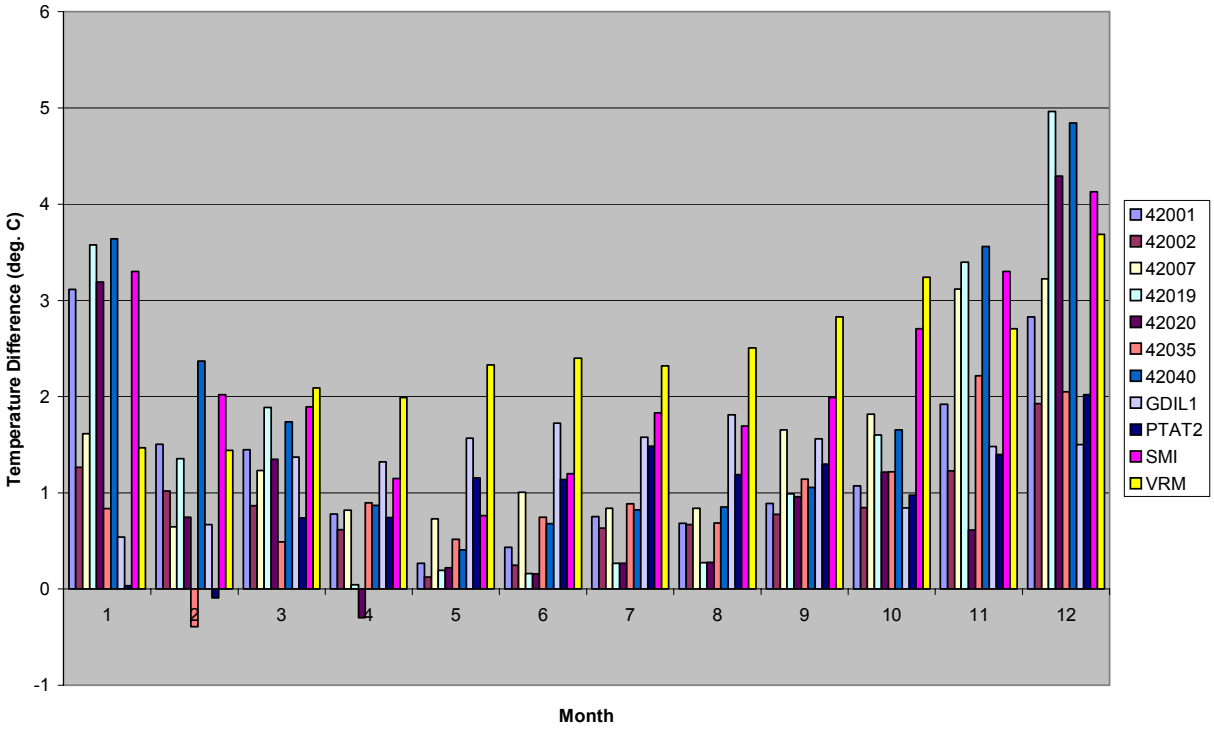

Figure 5. Monthly average sea-skin temperature minus air temperature for May 1998 through October 2001.

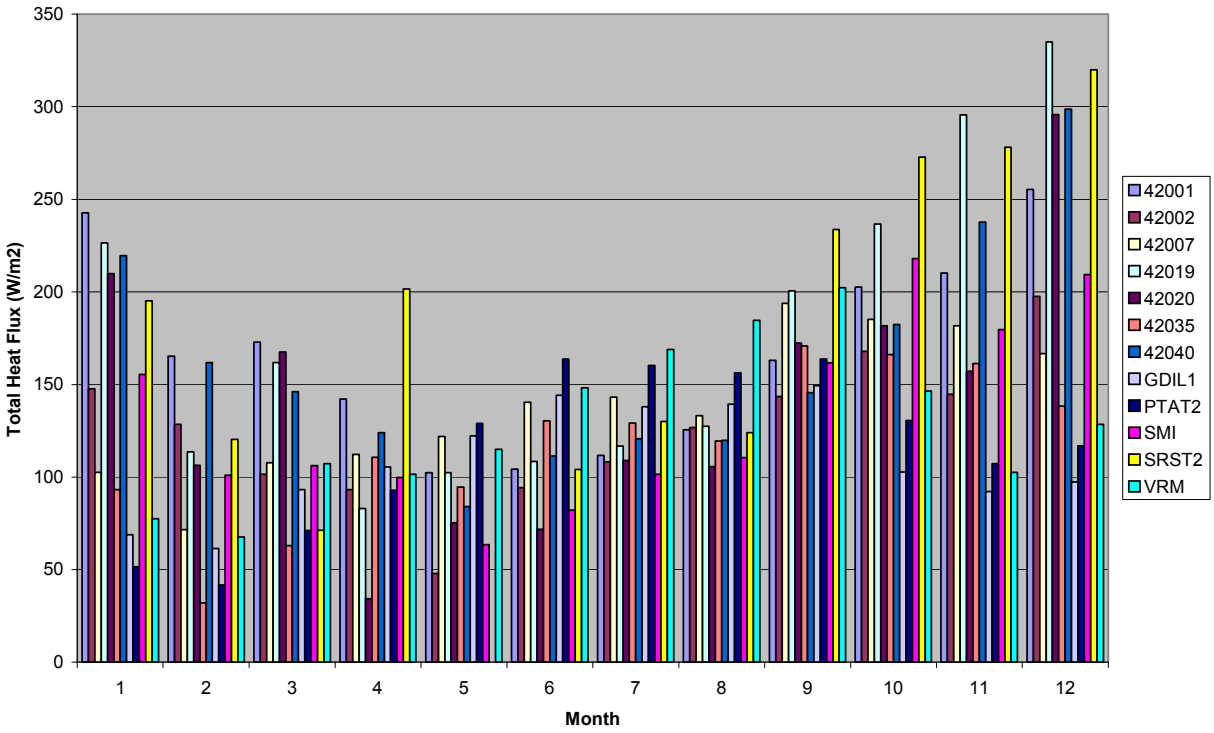

Figure 6. COARE monthly average of total heat fluxes (sensible plus latent) for May 1998 through October 2001.

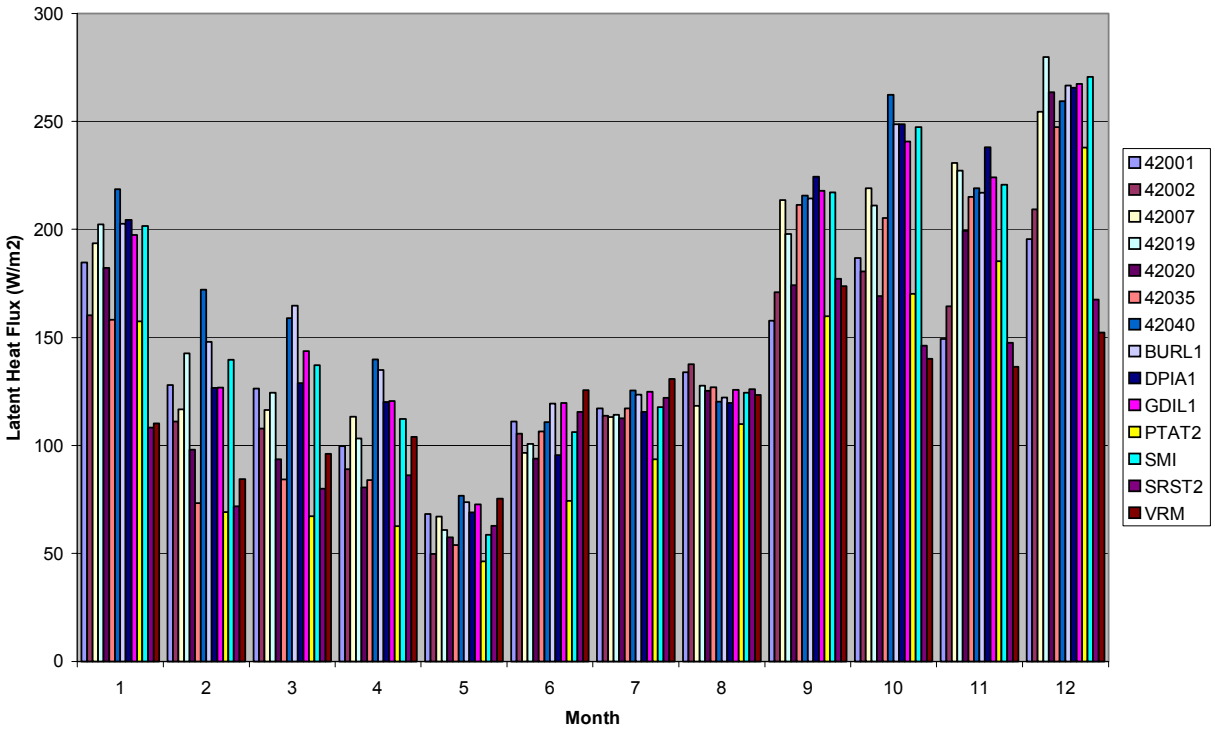

Figure 7. ETA monthly average latent heat fluxes for May 1998 through October 2001, for the 6- to 12-hour forecast.

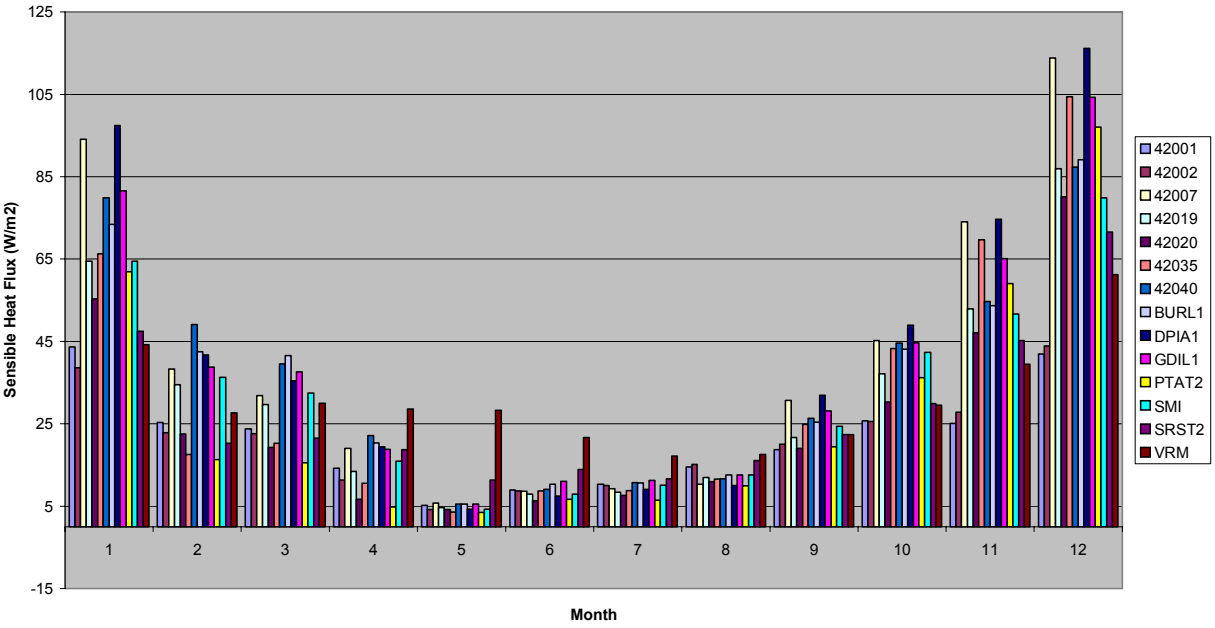

Figure 8. ETA monthly average sensible heat fluxes for May 1998 through October 2001, for the 6- to 12-hour forecast.

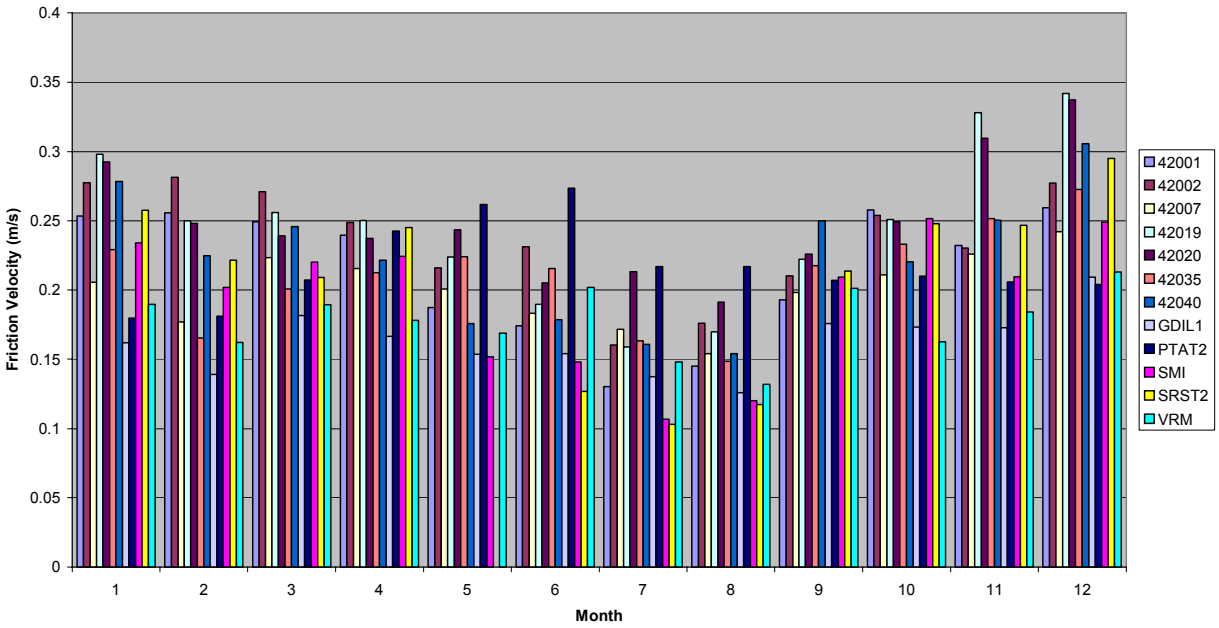

Figure 9. COARE monthly average friction velocity for May 1998 through October 2001.

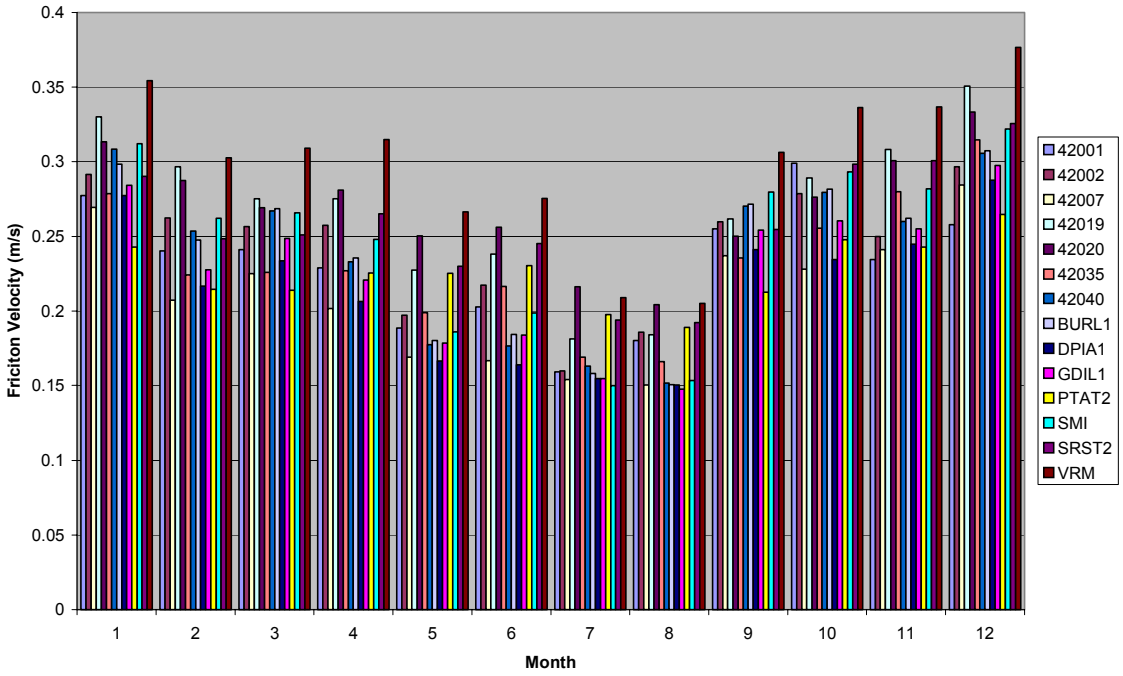

Figure 10. ETA monthly average friction velocity for May 1998 through October 2001, for the 6- to 12-hour forecast.

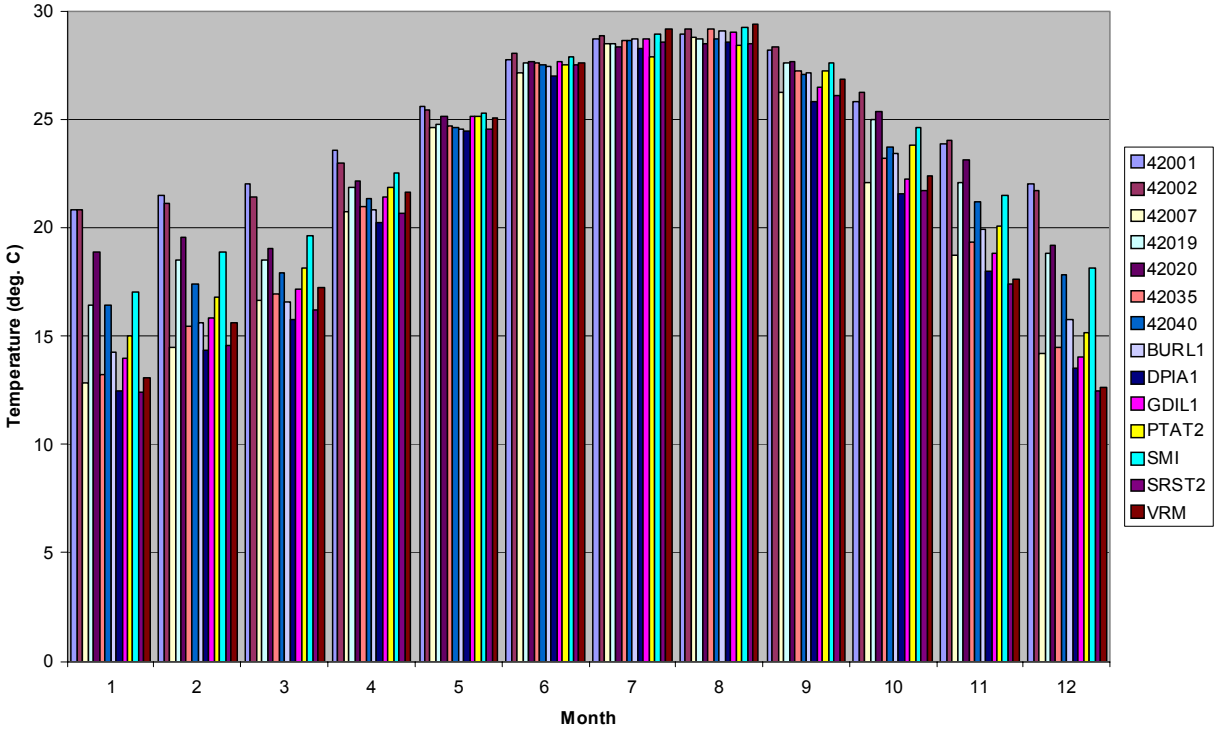

Figure 11. Observed monthly average air temperature for May 1998 through October 2001.

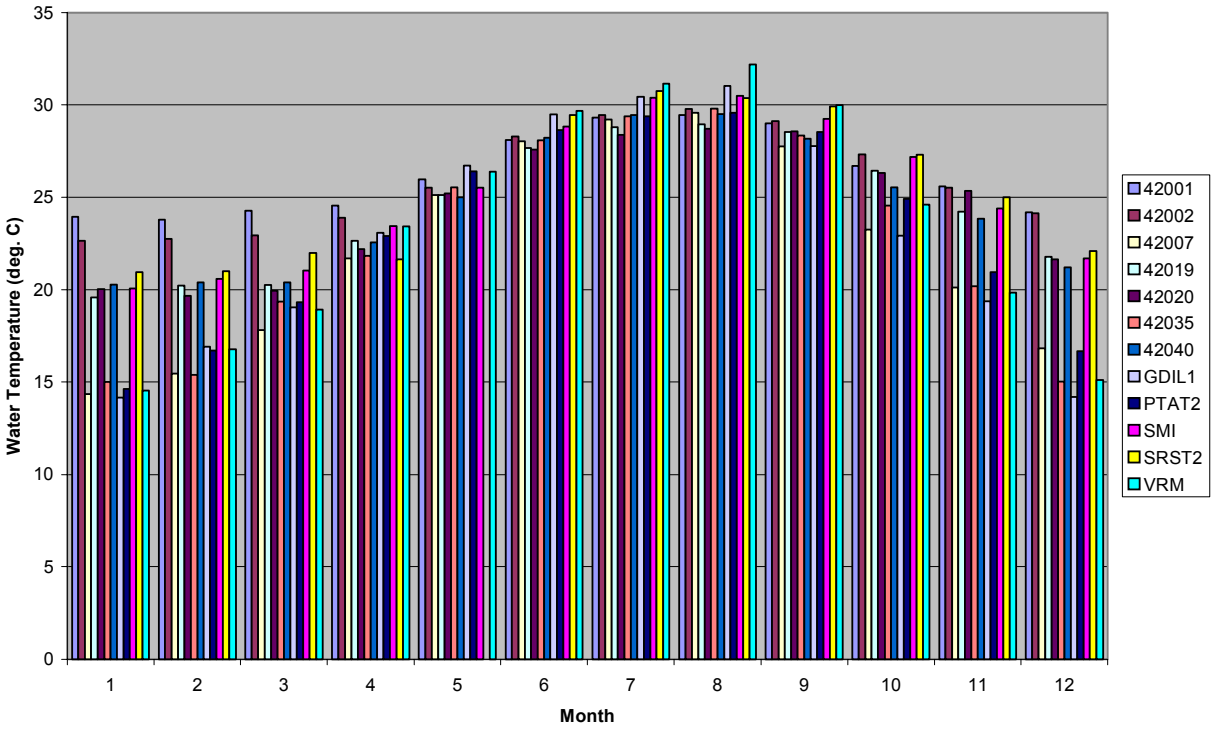

Figure 12. Observed monthly average sea-skin temperature for May 1998 through October 2001.

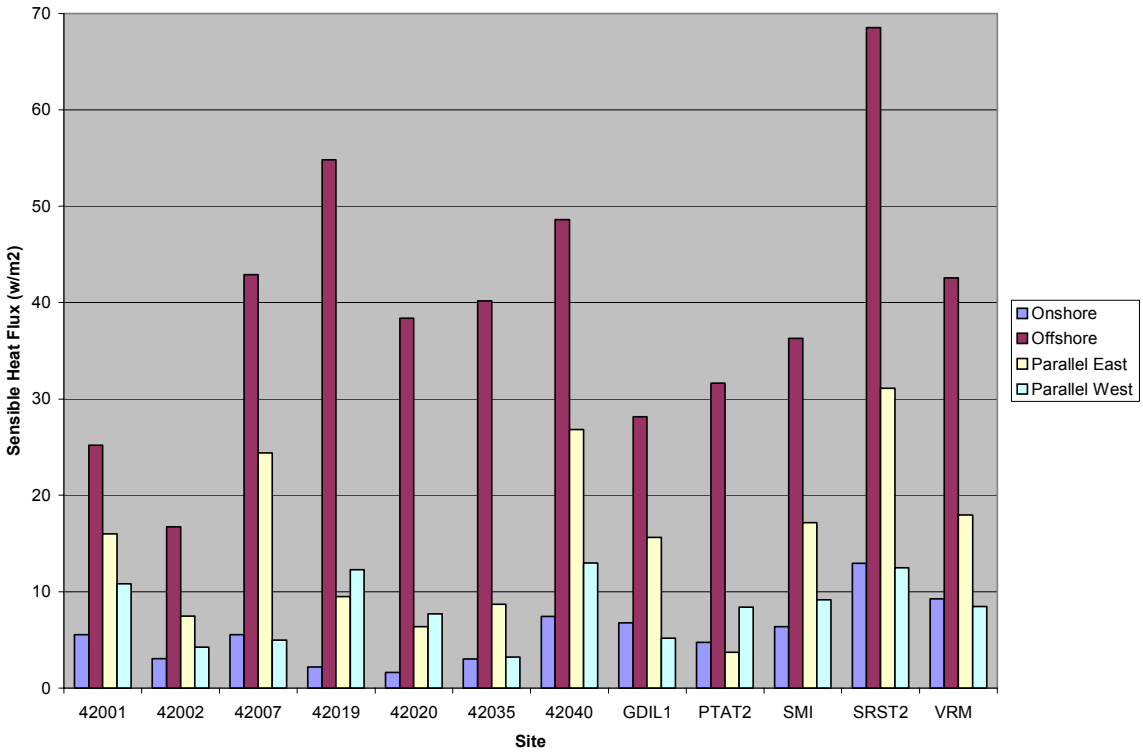

Figure 13. COARE average sensible heat fluxes by general flow direction for May 1998 through October 2001.

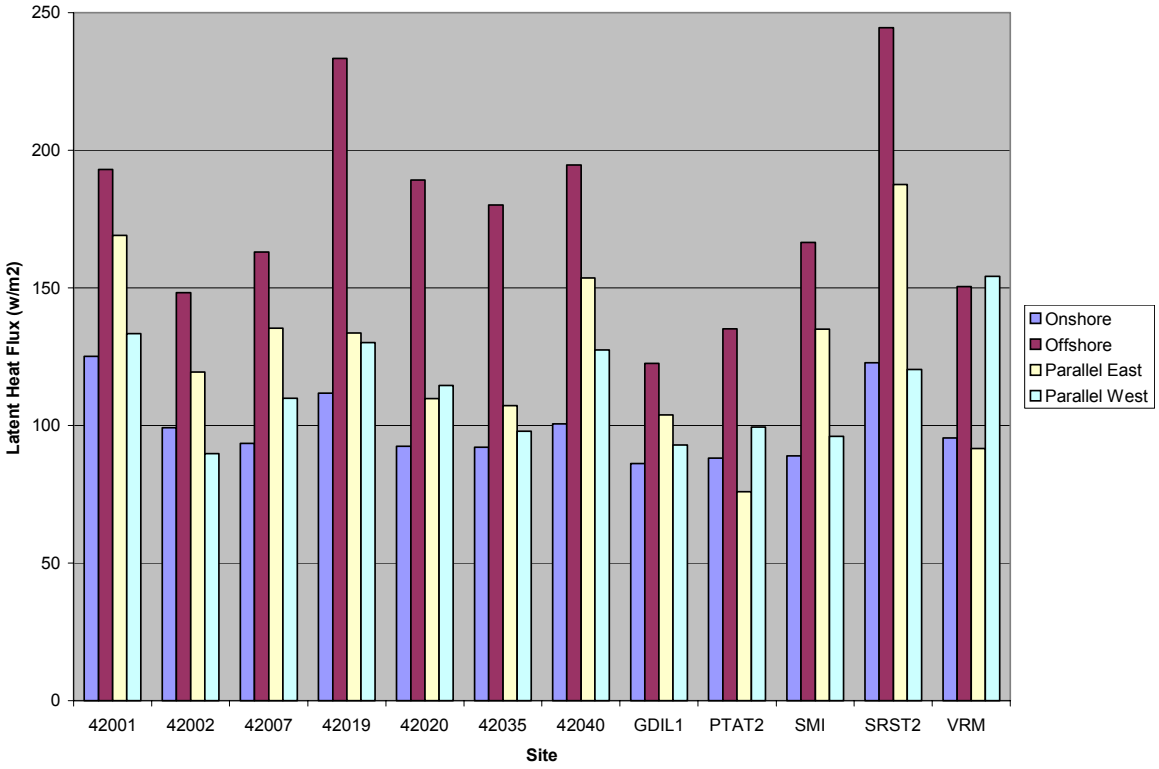

Figure 14. COARE average latent heat fluxes by general flow direction for May 1998 through October 2001.

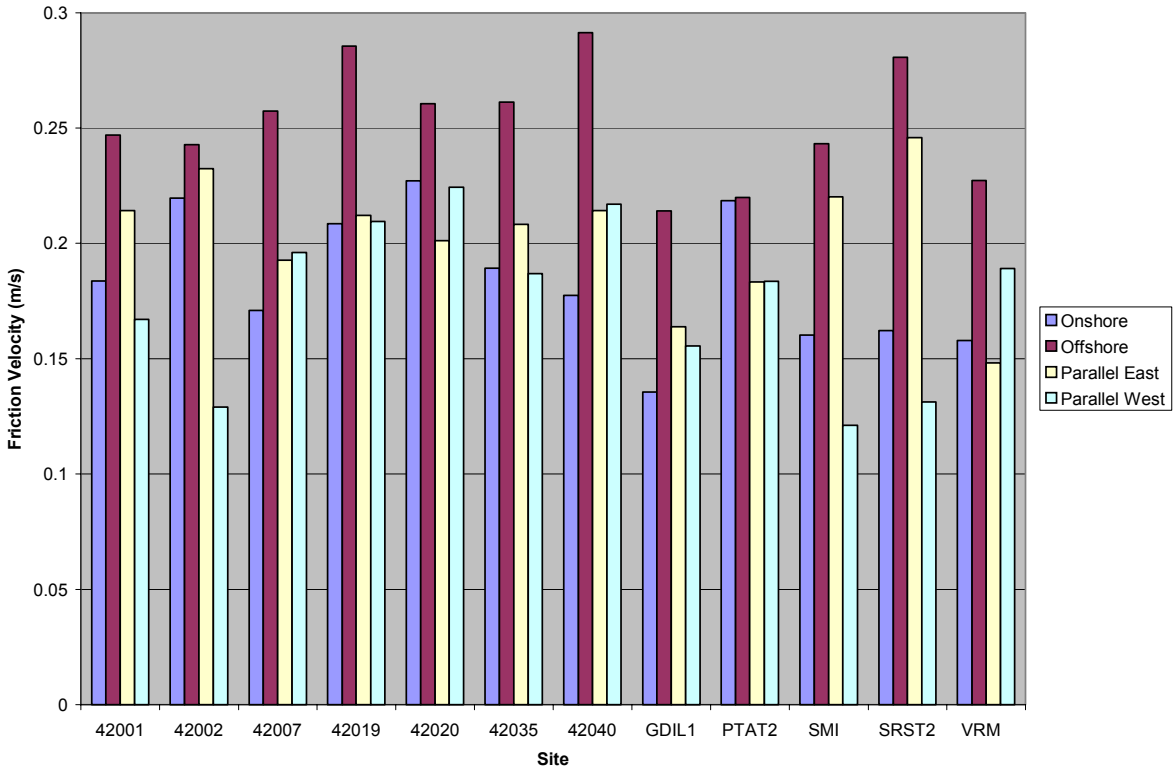

Figure 15. COARE average friction velocity by general flow direction for May 1998 through October 2001.

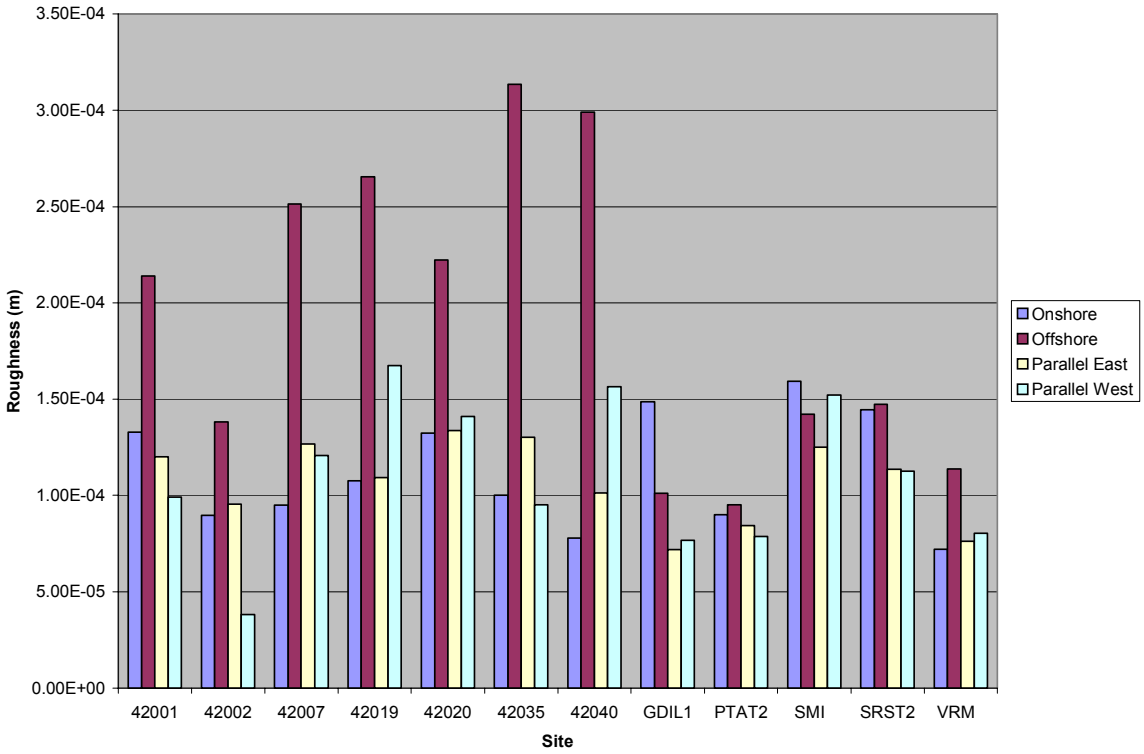

Figure 16. COARE average surface roughness by general flow direction for May 1998 through October 2001.

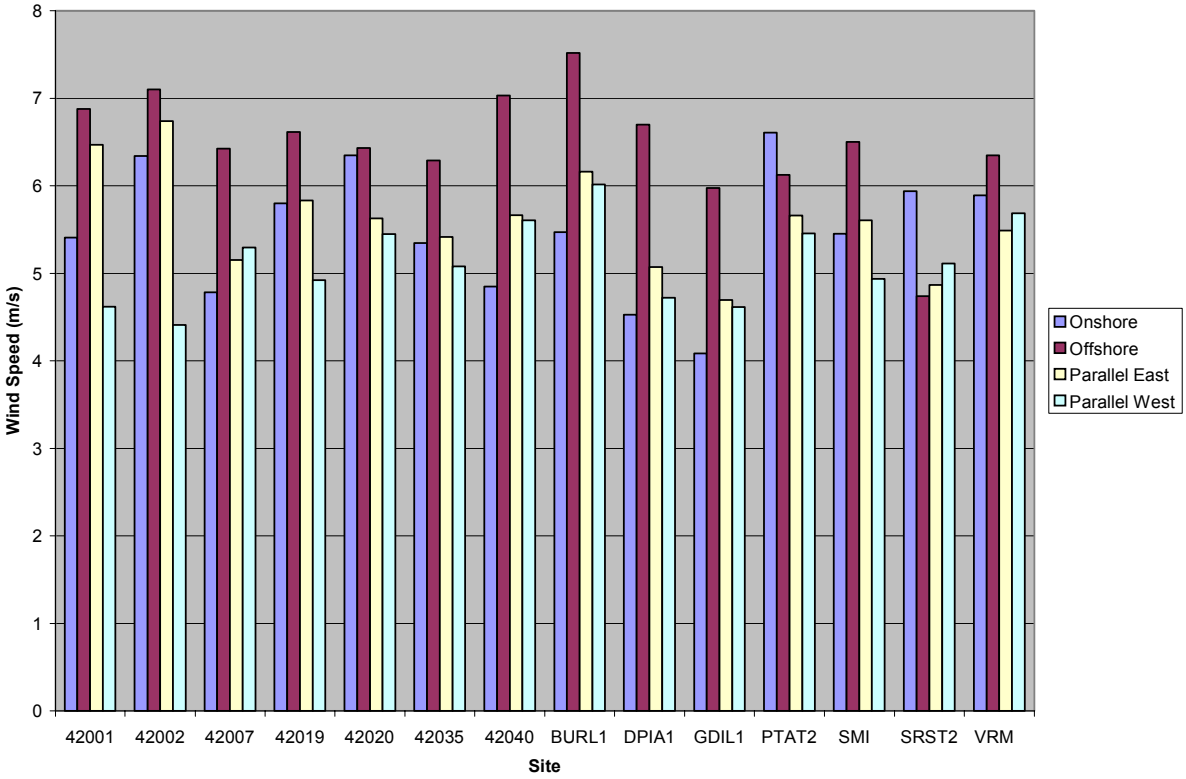

Figure 17. Observed average wind speed by general flow direction for May 1998 through October 2001.

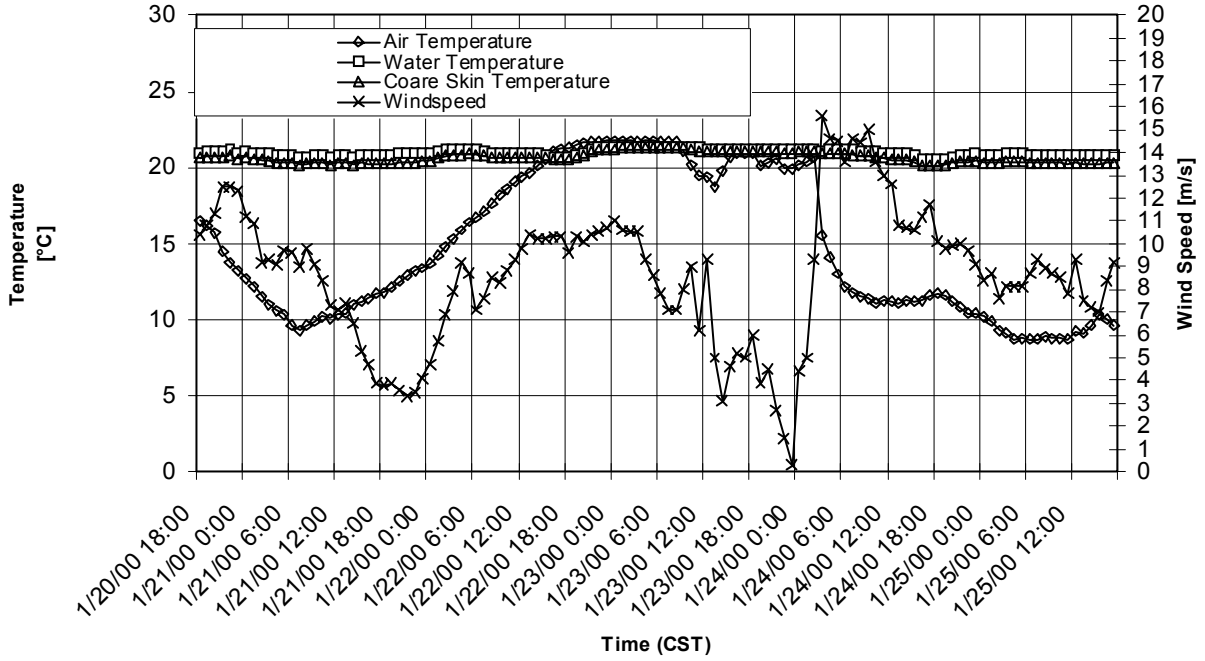

Figure 18. Observed wind speed, ambient air temperature, 0.6-m underwater temperature, and COARE 2.6bw derived skin temperature at buoy 42040 for January 20-25, 2000 at 1800 CST.

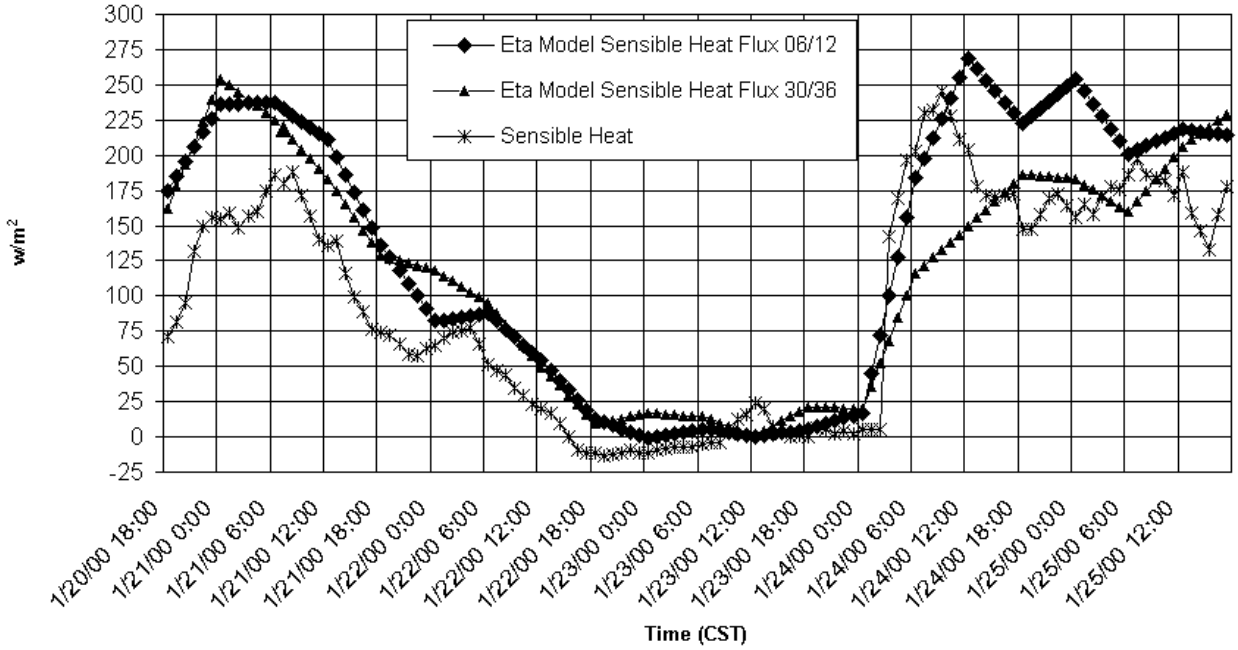

Figure 19. COARE 2.6bw derived sensible heat flux at buoy 42040 and Eta model sensible heat flux simulations for the 6- and 12-hour (06/12) and 30- and 36-hour (30/36) forecast periods near buoy 42040 for January 20-25, 2000 at 1800 CST. Note that the Eta model simulations are available every six hours at 0000, 0600, 1200, and 1800, and have been interpolated to hourly values.

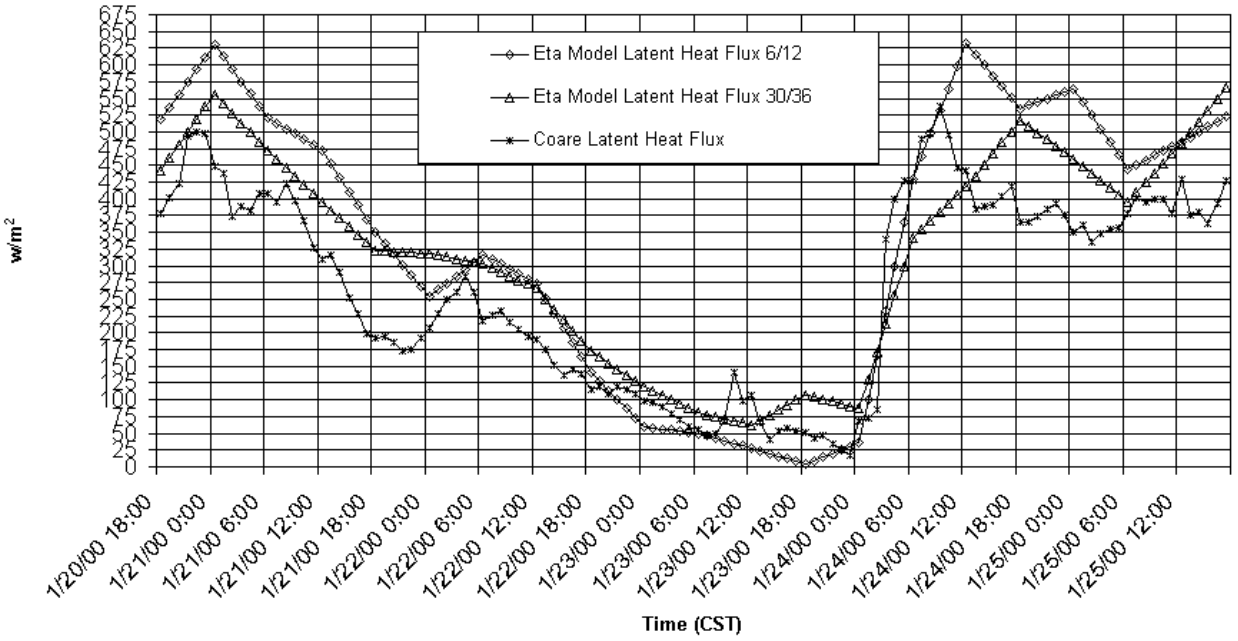

Figure 20. COARE 2.6bw derived latent heat flux at buoy 42040 and Eta model latent heat flux simulations for the 6- and 12-hour (06/12) and 30- and 36-hour (30/36) forecast periods near buoy 42040 for January 20-25, 2000 at 1800 CST. Note that the Eta model simulations are available every six hours at 0000, 0600, 1200, and 1800, and have been interpolated to hourly values.